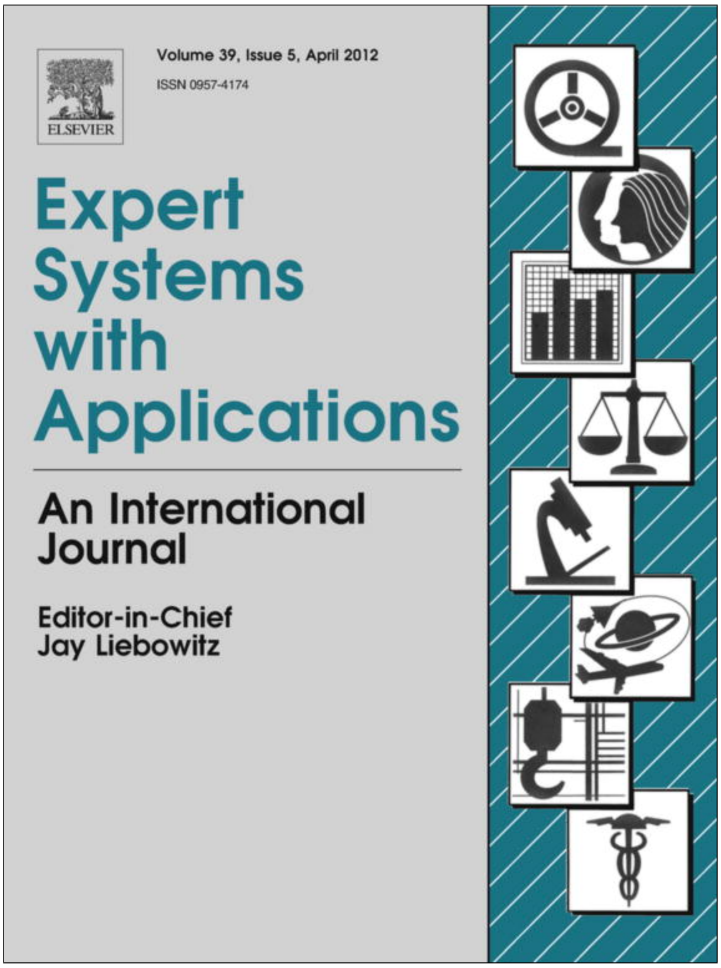
Volume 39, Issue 5, April 2012
ISSN 0957-4174
ELSEVIER
Expert Systems with Applications
An International Journal
Editor-in-Chief
Jay Liebowitz

Expert Systems with Applications 39 (2012) 5367–5375

Contents lists available at SciVerse ScienceDirect

Expert Systems with Applications

journal homepage: www.elsevier.com/locate/eswa

Temporary short circuit detection in induction motor winding using combination of wavelet transform and neural network

D.A. Asfani [a,b,*], A.K. Muhammad [c], Syafaruddin [d], M.H. Purnomo [b], T. Hiyama [a]

[a] Department of Computer Science and Electrical Engineering, Kumamoto University, 2-39-1 Kurokami, Kumamoto 860-8555, Japan
[b] Department of Electrical Engineering, Intitut Teknologi Sepuluh Nopember, 60111 Surabaya, Indonesia
[c] Faculty of Electrical and Electronic Engineering, Universiti Tun Hussein Onn Malaysia, 86400 Parit Raja, Johor, Malaysia
[d] Department of Electrical Engineering of Universitas Hasanuddin, 90245 Tamalanrea-Makassar, Indonesia

ARTICLE INFO

Keywords:
Temporary short circuit
Induction motor winding
Wavelet transform
Neural network

ABSTRACT

Monitoring system for induction motor is widely developed to detect the incipient fault. Such system is desirable to detect the fault at the running condition to avoid the motor stop running suddenly. In this paper, a new method for detection system is proposed that emphasizes the fault occurrences as temporary short circuit in induction motor winding. The investigation of fault detection is focused on the transient phenomena during starting and ending points of temporary short circuit. The proposed system utilizes the wavelet transform for processing the motor current signal. Energy level of high frequency signal from wavelet transform is used as the input vriable of neural network which works as detection system. Three types of neural networks are developed and evaluated including feed forward neural network (FFNN), Elman neural network (ELMNN) and radial basis functions neural network (RBFNN). The results show that ELMNN is the most simply and accurate system that can recognize all of unseen data test. Laboratory based experimental setup is performed to provide real-time measurement data for this research.

1. Introduction

Induction motors are the most widely used rotary machines in industrial sector for electrical to mechanical energy conversion due to the high development of operation control of motor system. About 70% of the industrial applications utilize induction machines and because of this trend they consume more than 50% of an industrialized power generating capability (Cusido, Rosero, Ortiga, Garcia, & Romeral, 2006). However, the induction motors are very easy to be damaged during their operations. In some industrial processes, the induction motors are often installed in the hostile environment that may be easily led to the deterioration. Moreover, several problems may occur during operation because of thermal, mechanical and electrical stresses. In spite of their reliability and robustness, they do occasionally fail with unpredictable downtime that causes obvious cost maintenance (Niu et al., 2008). Some studies and site surveys show that 30–40% of induction motor failures are caused by stator winding breakdown because of lamination breakdown or stator winding defects (Siddique, Yadava, & Singh, 2005). In order to avoid huge risk of loss production, obvious cost maintenance and also operator safety of industrial process because of sudden stop of motor failure, predictive maintenance and fault diagnosis is highly needed. For this task, on-line monitoring is commonly equipped to detect the fault symptoms. In recent years, research and development methods for on-line monitoring and incipient fault detection for induction motor, especially for winding failure have been receiving wide attention. Mostly, motor current signal has pretty similar pattern as sinusoidal signal and occasionally changes gradually due to mechanical load changes. Therefore, the similarity of sinusoidal pattern results in the similarity of RMS value of the current. However, motor current signal trend is rapidly changed when the fault or short circuit occurs. Detection incipient fault such as small current short circuit in winding was proposed (D'angelo et al., 2011). Short circuit is detected by using combination of fuzzy system and Bayesian change point that use current signal as the input variable detection. Motor current pattern is modeled as time series based fuzzy-neural network and incipient fault is successfully detected by using characterize change point in that model. Another proposed model for fault diagnosis called neuro multi-step ahead predictor was presented (Kim & Parlos, 2002). This proposed model combines model based and measurement based system. Residual signal is named to the signal that obtained from differentiate of measurement and prediction signal. Residual signal together with harmonics of

* Corresponding author at: Department of Computer Science and Electrical Engineering, Kumamoto University, 2-39-1 Kurokami, Kumamoto 860-8555, Japan. Tel.: +81 8039091404; fax: +81 963423630.
E-mail address: anton_dimas@yahoo.com (D.A. Asfani).

0957-4174/$ - see front matter © 2011 Elsevier Ltd. All rights reserved.
doi:10.1016/j.eswa.2011.11.048

current signal is used as detection variable to distinguish normal and faulty conditions. The most popular method to detect the fault at induction machine is known as motor current signature analysis (MCSA). This method utilizes the frequency pattern of motor current to detect availability of faults. This method, however, does not always clearly detect the fault when the speed or load torque is not constant due to the non-stationary signal. In order to overcome this problem, Fourier transform is combined with wavelet transforms and power spectral density (PSD) techniques (Cusido, Romeral, Ortega, Rosero, & Garcia Espinosa, 2008). Fault in induction motor may affect in many measurement parameters of motor such as current, flux and vibration, but the relationship of those parameters and the fault type are different in case by case. Such relationship is more complex in different loading cases or other operation conditions. Those complexity of motor faults let the researchers to apply the non-linear and adaptive solution to solve the problem. In order to obtain the significant parameter for detection, some methods for classification and signal processing are used. Case based-reasoning (CBR) which is known as a technique uses implicit knowledge from previous case and experience to guide solving problem combined with Petri nets (PNs) is used to diagnosis induction motor faults. This system is capable to add the new cases and conducting revision to improve system capability (Yang, Jeong, Oh, & Tan, 2004). In other approaches, Fourier transforms combined with classification and regression tree (CART) as classification parameter and adaptive neuro fuzzy inference system (ANFIS) as an adaptive detection system are utilized for fault diagnosis system (Tran, Yang, Oh, & Tan, 2009). Similar with detection system and fault diagnosis, on-line monitoring system for induction motor has reached excellent progress in their development methods. On-line monitoring based on motor current measurement was proposed (Acosta, Verucchi, & Gelso, 2006). Frequency spectrum analysis accompanied with the non-invasive technique which called the extended Park's vector approach is used as detection system. The later techniques accurately detect the inter-turn short circuit. Another method is the simplified scheme for monitoring system based on spectrum analysis combined with fuzzy system (Rodriguez, Negrea, & Arkkio, 2008). In this scheme, the system is utilized by adaptive multistage filter to anticipate uncertainty noise signal. In order to optimize performance of this filter, several loading cases and noising input are trained. In this paper, a new method for on-line monitoring and fault detection system of induction motor winding are presented. The detection is emphasized on the transient phenomena during fault starting and ending points. This method is purposed to detect temporary short circuit in order to define the incipient of fault occurrence. This short circuit is specified as follow; temporary by means not permanently short circuit; low current that specified below 300% current rating; and non periodic occurrences. Beside the proposed method has simple calculation and implementation, it is also capable to detect temporary short circuit and to provide information about when the short circuit occurs accurately, such as at the fault starting and ending points. Combination of wavelet transform and neural network (NN) is designed to do this task. Wavelet transform is used as signal processing to obtain precious signal that contains the fault information. In this task, second level Haar wavelet transform is selected because it has simple calculation method and is capable to extract the needed information. Energy level of high frequency signal from wavelet transform is selected as the input signal of detection system. The optimal detection system configuration is developed and selected from three types of neural network, including feed forward neural network (FFNN), Elman neural network (ELNN) and radial basis function neural network (RBFNN). Several cases of temporary fault are tested and investigated in the laboratory experiment and current signal that contains the fault phenomena is recorded.

2. Configuration of proposed method

In this section, the proposed method using energy level of high frequency signal extracted by discrete wavelet transform and neural network configuration for detection system will be explained. The flowchart of our proposed method is shown in Fig. 1. In this figure, motor current signal is measured and converted to digital data. There are three periods of sampling $T1$, $T2$ and $T3$ used in the monitoring signal and each incoming signal will be simultaneously processed in the sequent step. Furthermore, each signal is filtered using second level Haar wavelet transform and it may result high and low frequency; but only the high frequency signal is used for further processing. After this step, the energy level all of three high frequency signals are obtained and the results are $x1$, $x2$, and $x3$. Finally, the last step is the fault detection system which consists of neural network system with the input variables are $x1$, $x2$ and $x3$ simultaneously.

2.1. Discrete wavelet transform

Wavelet transform (WT) is known as an alternative method to analyze non-stationary signal beside the conventional method, short-time Fourier transform (STFT). When STFT is applied, the non-stationary signal is divided into small windows of equal time and Fourier transform is then applied to the time segment being examined. As the wide of windows function decreases, the greater time location is acquired but it will consider smaller portion of frequency information. On the other hand, when the windows function is increased, more accurate frequency information will increase but

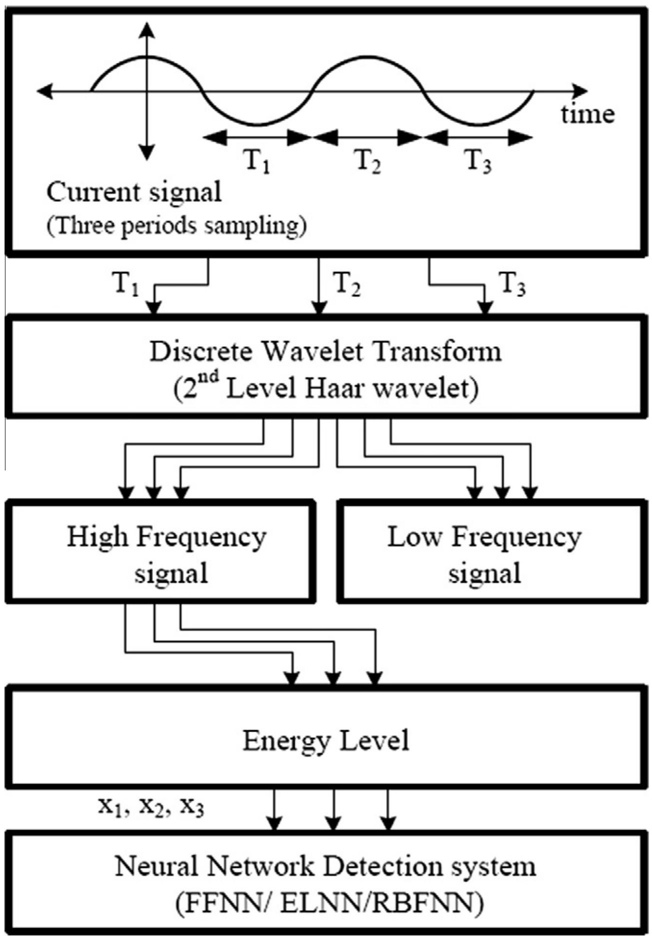

Fig. 1. Flowchart proposed method.

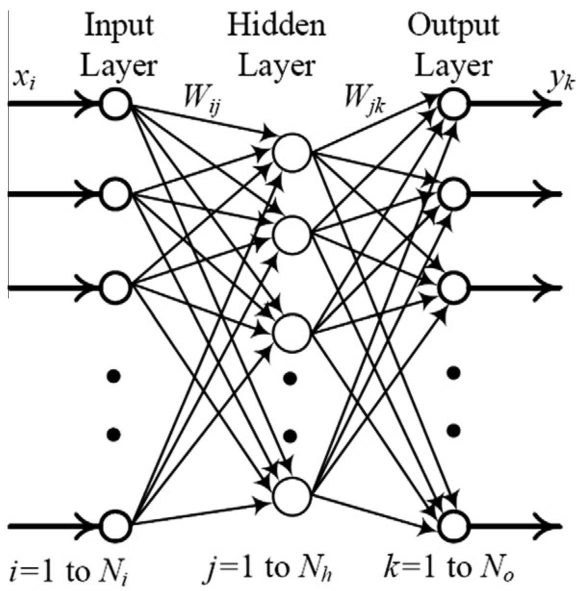

Fig. 2. Feedforward neural network.

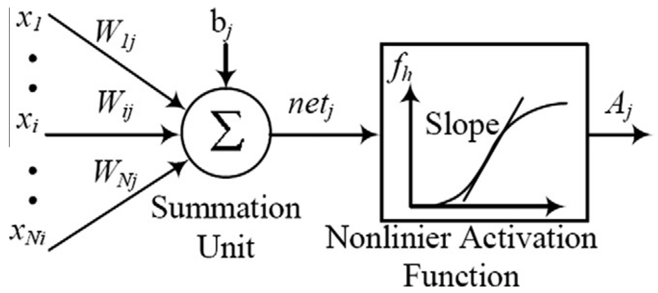

Fig. 3. Hidden layer.

the ability of method to determine the time when transient occur is decreased (Niu et al., 2008). In order to overcome the shortcoming of STFT, wavelet transform is introduced as an alternative solution to analyze the non-stationary signal that provides both frequency and time information simultaneously (Burrus, Gophinath, & Guo, 1998). Wavelet function is expressed using $\psi(\cdot)$ and should be satisfying two basic properties as follows, the integral of $\psi(\cdot)$ is zero (1), and the square of $\psi(\cdot)$ integrates to unity (2)

$$\int_{-\infty}^{\infty} \psi(u)du = 0 \tag{1}$$

$$\int_{-\infty}^{\infty} \psi^2(u)du = 1 \tag{2}$$

Wavelet transform consists of two functions, scaling functions, $\phi(t)$ which is deducted by father wavelet and wavelet function, $\psi(t)$ deducted by mother function. These functions are mathematically expressed as follows:

$$\phi_{j,k}(t) = 2^{j/2}\phi(2^j t - k) \tag{3}$$

$$\psi_{j,k}(t) = 2^{j/2}\psi(2^j t - k) \tag{4}$$

Using these functions, some signals can be formed as low and high frequency signals, $c_{j,k}$ and $d_{j,k}$ respectively and reconstructed to the origin signal

$$c_{j,k} = \int_{-\infty}^{\infty} f_j(t) * \phi_{j,k}(t)dt \tag{5}$$

$$d_{j,k} = \int_{-\infty}^{\infty} f_j(t) * \psi_{j,k}(t)dt \tag{6}$$

2.1.1. Haar wavelet

Haar wavelet is the oldest and simplest of all wavelets. The Haar wavelet has been known for hundred years and it has been used to solve various fields such as mathematics and engineering. The Haar wavelet and scaling function are defined as (7) and (8), respectively

$$\psi(t) = \begin{cases} 1 & \text{for } t \in \left[0, \frac{1}{2}\right] = 0 \\ -1 & \text{for } t \in \left[\frac{1}{2}, 1\right] = 0 \\ 0, & \text{otherwise} \end{cases} \tag{7}$$

$$\phi(t) = \begin{cases} 1 & \text{for } 0 < t < 1 \\ 0, & \text{otherwise} \end{cases} \tag{8}$$

Based on Haar wavelet and scaling function, Haar wavelet decomposition of digital signal $x[k]$ at level j is described as in (9) as follows:

$$c_j(k), d_j(k) = W_T[n]x[n] \tag{9}$$

Low frequency signal $c_j(k)$ and high frequency signal $d_j(k)$ are obtained by simple convolution the digital signal $x[n]$ with wavelet transform $W_T[n]$. For Haar purpose, the wavelet transform can be defined as follows:

$$W_T[n] = \begin{bmatrix} \frac{1}{\sqrt{2}} & \frac{1}{\sqrt{2}} \\ \frac{1}{\sqrt{2}} & -\frac{1}{\sqrt{2}} \end{bmatrix} \tag{10}$$

Simple convolution of Haar wavelet is expressed in (11), where c_{j-1} can be the original signal

$$\begin{bmatrix} c_j(k) \\ d_j(k) \end{bmatrix} = \frac{1}{\sqrt{2}} \begin{bmatrix} 1 & 1 \\ 1 & -1 \end{bmatrix} \begin{bmatrix} c_{j-1}(2k) \\ d_{j-1}(2k+1) \end{bmatrix} \tag{11}$$

From (11) we can obtain the low frequency signal as $c_j(k)$ and high frequency signal $d_j(k)$ as follows:

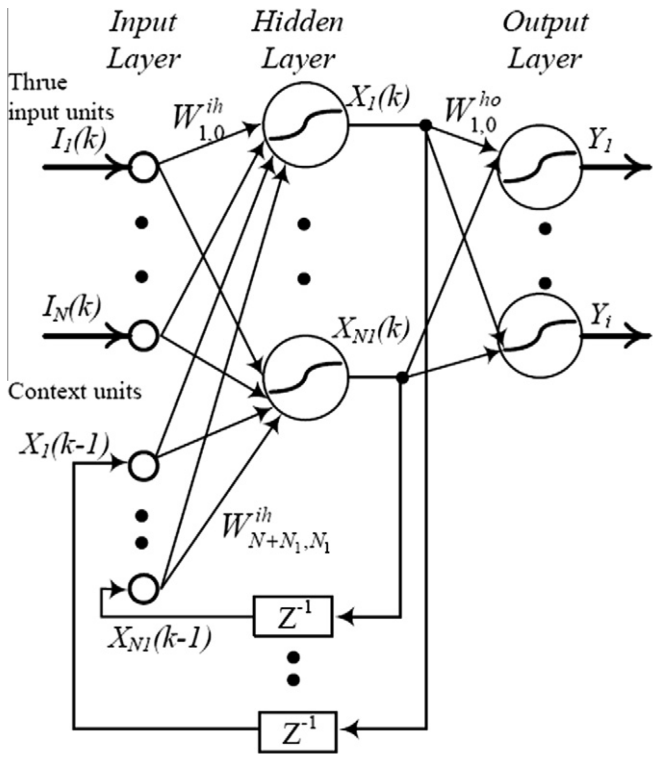

Fig. 4. Elman neural network.

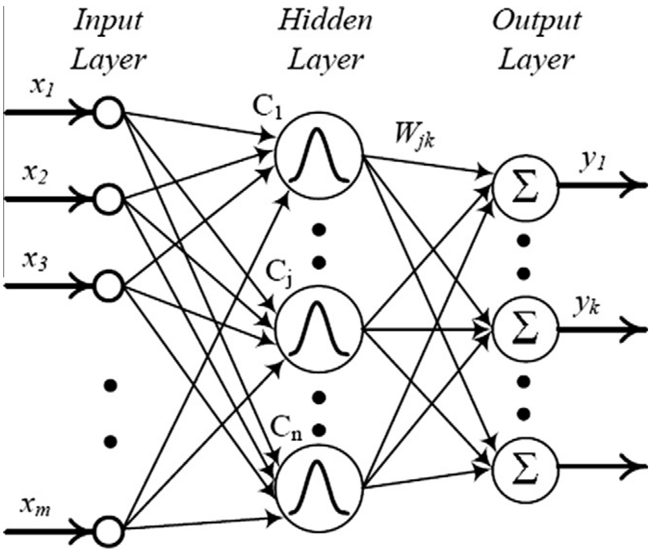

Fig. 5. Radial basis function neural network.

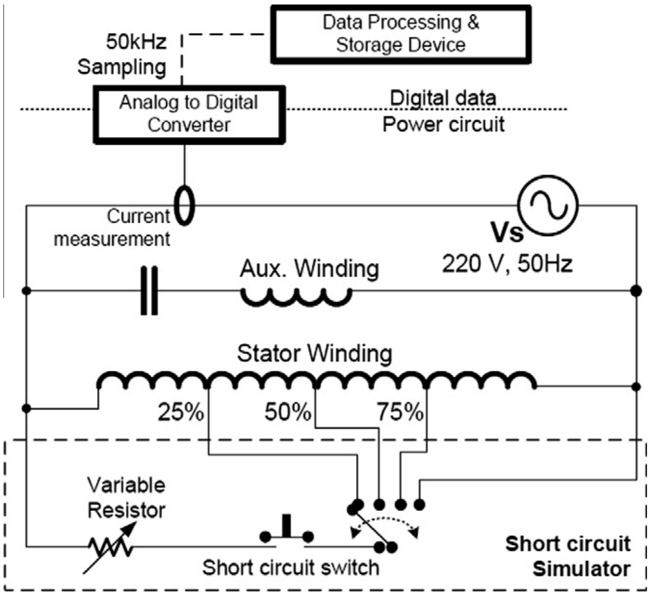

Fig. 6. Experimental scheme.

$$c_j(k) = \frac{1}{\sqrt{2}}(((1)c_{j-1}(2k)) + ((1)c_{j-1}(2k+1))) \quad (12)$$

$$d_j(k) = \frac{1}{\sqrt{2}}(((1)c_{j-1}(2k)) + ((-1)c_{j-1}(2k+1))) \quad (13)$$

The first level decomposition of Haar wavelet transform is defined by substitute $j = 1$ in (14) and (15)

$$c_1(k) = \frac{1}{\sqrt{2}}((c_0(2k)) + (c_0(2k+1))) \quad (14)$$

$$d_1(k) = \frac{1}{\sqrt{2}}((c_0(2k)) - (c_0(2k+1))) \quad (15)$$

For the second level $j = 2$ the transformation can be obtained as follows:

$$d_2(k) = \frac{1}{\sqrt{2}}((c_1(2k)) + (c_1(2k+1))) \quad (16)$$

Substitute $c_1(2k)$ and $c_1(2k+1)$ to (16); the high frequency signal of second level decomposition can be calculated from the original signals

$$d_2(k) = \frac{1}{\sqrt{2}}(c_0(4k) + c_0(4k+1) - c_0(4k+2) - c_0(4k+3)) \quad (17)$$

2.1.2. Energy level

In this paper, the energy of high frequency signal is calculated as follows:

$$e = \sum_{n=1}^{n=k} |y_{high}[n]|^2 \quad (18)$$

Energy values are used as input variables for developed artificial neural network which works as detection system for the temporary fault in induction motor winding.

2.2. Artificial neural network (ANN)

During the last two decades, there has been a substantial increase in the interest on ANNs. ANNs have been successfully employed in solving complex problems in various fields (Kirmaci, Menlik, & Ozdemir, 2010). In this paper there are three types of neural network are investigated to obtain the most suitable system for detecting temporary fault.

2.2.1. Feed forward neural network (FFNN)

A feed forward neural network consists of a number of simple neuron which organized in *layers*. Every neuron or node in a layer is connected with all the nodes in the previous layer. Each connection may have a different value of *weight* or strength. The weights on these connections represent the knowledge of a network. Data passes through the network until it arrives at the outputs. There is no feedback between layers so it called *feedforward* neural networks. The architecture of a FFNN with one hidden layer is shown in Fig. 2.

The input layer consists of Np inputs. Each pth input is connected to the each qth node of the hidden layer by a weighting factor, W_{pq}. Each node in the hidden layer performs a nonlinear transformation of its weighted input signals. The model of unit q in the hidden layer is shown in Fig. 3.

The output of this neuron can be formulated as:

$$A_q = f_h(net_q) \quad (19)$$

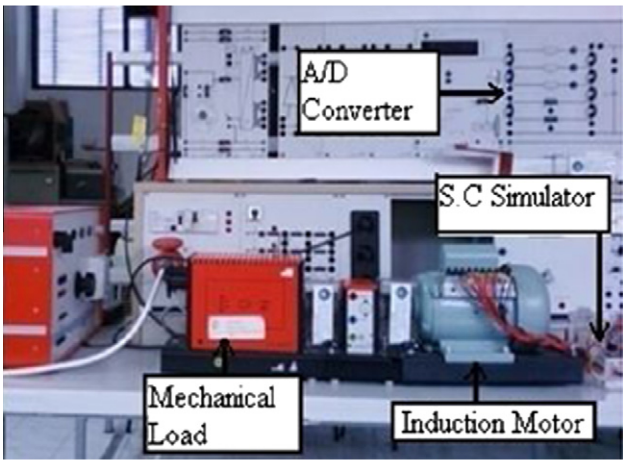

Fig. 7. Experimental set up.

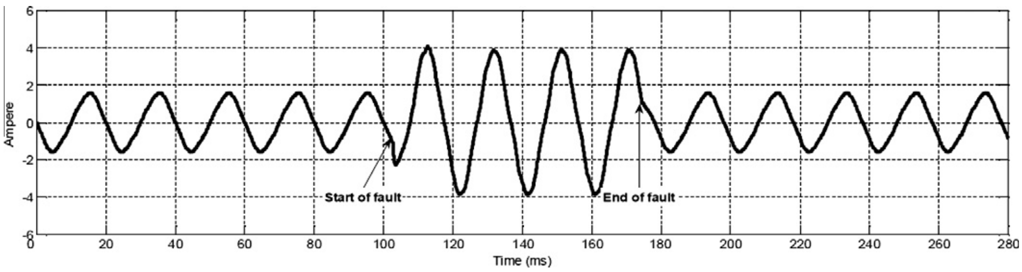

Fig. 8. Current signal during temporary fault.

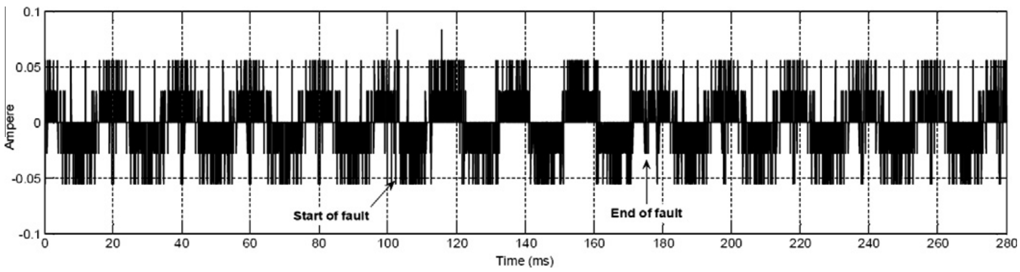

Fig. 9. High frequency signal using 1st level Haar wavelet transform.

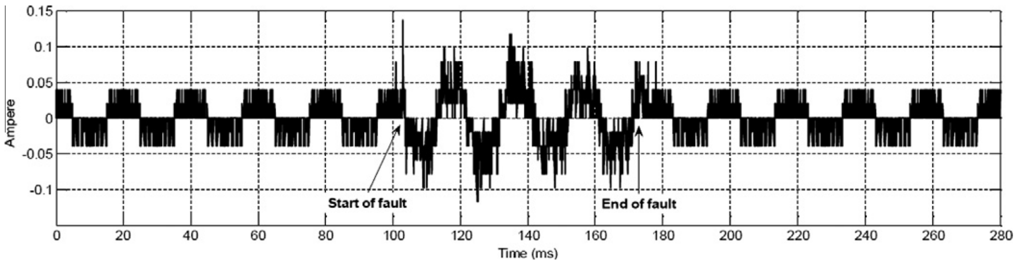

Fig. 10. High frequency signal using 2nd level Haar wavelet transform.

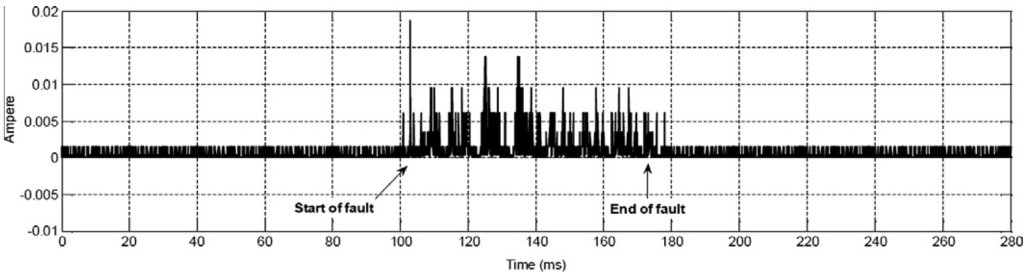

Fig. 11. High frequency signal square using 2nd level Haar wavelet transform.

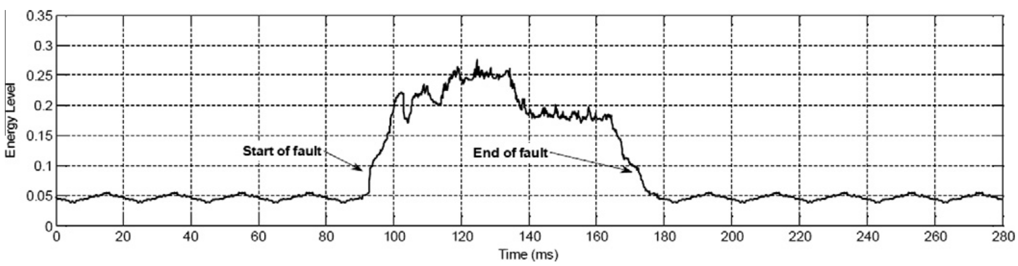

Fig. 12. Energy level.

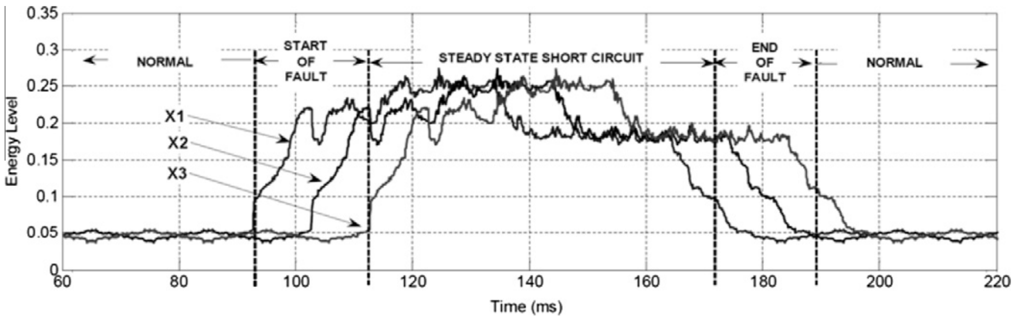

Fig. 13. Input variable neural network

where f_h is a nonlinear activation function in the hidden layer which can be a bounded monotonic function such as hyperbolic tangent, sigmoid, semi-linear, etc. During training process, only the value of its slope is varied. Input of f_h is net_q that can be formulated as:

$$net_q = \sum_{p=1}^{N_p} W_{pq} x_p + b_q \tag{20}$$

where x_p is the input of unit p in the input layer; W_{pq} is the weighting factor between neuron p of the input layer and neuron q of the hidden layer, respectively; and b_q is the bias term of the neuron. All the weighting factors and bias terms are adjusted during the training process. The structure of the FNN output layer is similar to the hidden layer with the exception that the inputs of the output layer are the outputs of the hidden layer. The output of neuron r in the output layer can be formulated as:

$$y_r = f_o(net_r) \tag{21}$$

where f_o is the nonlinear activation function in the output layer, net_r is equal to:

$$net_r = \sum_{p=1}^{N_h} W_{qr} A_q + b_r \tag{22}$$

and W_{qr} is the weighting factor between neuron q in the hidden layer and neuron r in the output layer (Sharif & Taylor, 2000).

2.2.2. Feed forward neural network (FFNN)

Unlike FFNN, Elman neural network architecture considers information about past data in recurrent connection which called context unit. Elman network configuration can be seen in Fig. 4. The function learnt by the network can be based on the current inputs plus a record of the previous states and outputs of the network. The Elman neural network is capable of providing the standard state-space representation for dynamic systems. This is the reason why this network architecture is utilized as a recurrent neural equalizer.

The Elman network has three layers, input, hidden and output. In the hidden layer and output layer nodes, the sigmoidal activation function is used (Koker, 2006). The expression for the hidden layer output is given as

$$X_q(k) = \frac{1}{\left(1 + exp\left(b_q^h(k) + \sum_{p=1}^{N} W_{pq}^{ph}(k) I_p(k) + \sum_{p=N+1}^{N+N_1} W_{pq}^{ph}(k) X_p(k-1)\right)\right)} \tag{23}$$

And the output as

$$Y_l(k) = \frac{1}{1 + exp\left(b_l^0(k) + \sum_{q=1}^{N_1} W_{ql}^{h0}(k) X_q(k)\right)} \tag{24}$$

where N_1 is the number of hidden nodes. $b_q^h(k)$ are the biases of the hidden node q, $W_{pq}^{ph}(k)$ are the weights from the input to the hidden layer, N_2 is the number of output nodes, $W_{qr}^{ho}(k)$ are the biases of the output layer nodes.

2.2.3. Radial basis function neural network (RBFNN)

Similar with two previous networks, an RBF neural network is consist of three layers; input layer, hidden layer and output layer. The network structure is shown in Fig. 5. The inputs $x_1, x_2, \ldots, x_m$, are connected to all neurons in the hidden layer. The hidden layer is composed of n number of RBFs and connected directly to all nodes in the output layer. A node in the hidden layer will result a greater output if the input pattern presented is close to the center point of RBF. The output node will decrease as the distance from the center increases. Therefore only the neurons or node whose centers are close to the input pattern will produce nonzero activation values to the input stimulus.

The basis function for the qth hidden node is often defined by a Gaussian exponential function calculated as follows:

$$h_q = h_{(\upsilon_q)} = exp\left(-\frac{\upsilon_q^2}{2\sigma_q^2}\right) \tag{25}$$

where $sigma_q$ is the width of the qth neuron, υ_q is usually selected by the Euclidean norm of the distance between the input and the neuron center calculated as follows:

Table 1
Data set.

Operation case	Training and validation		Testing	
	Number of cases	Variation (A)	Number of cases	Variation (A)
Normal	40	1, 1.3	10	1.2, 1.5
Steady state S.C	100	2.75; 3.2; 3.6; 3.8; 4	10	3.5; 4.5
Starting S.C	100	2.3;3.1; 3.25; 3.75; 4	15	3.1; 3.6; 3.86
Ending S.C	100	2.3; 3.1; 3.6; 3.8; 4	15	2.4; 3.2; 4.5
Total	340		50	

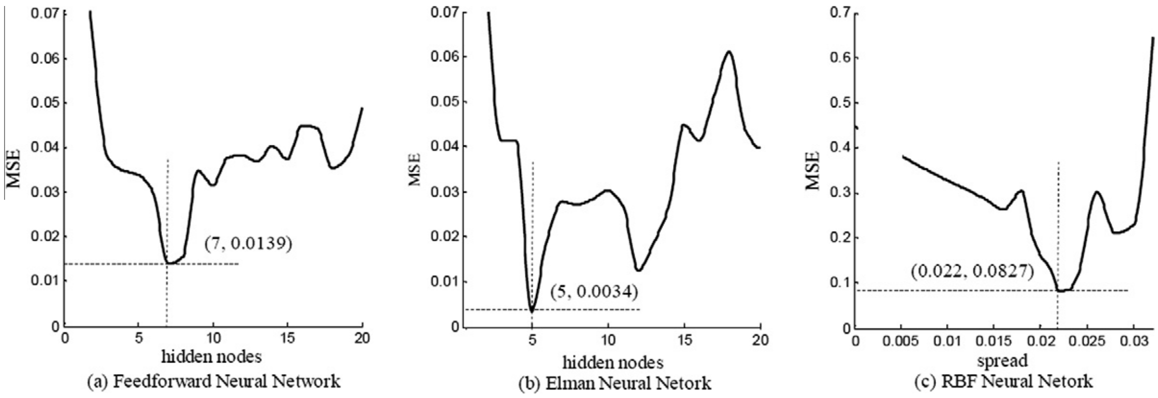

Fig. 14. Mean square error of testing data.

Table 2
Network performance.

Network	Data train		Data validation		Data test	
	SSE	MSE	SSE	MSE	SSE	MSE
FFNN	2.87×10^{-11}	2.11×10^{-14}	6.93×10^{-9}	5.10×10^{-12}	2.7721	0.0139
ELMNN	0.0775	5.70×10^{-5}	0.1122	8.25×10^{-5}	0.6835	0.0034
RBFNN	5.32×10^{-14}	3.91×10^{-17}	0.7131	5.24×10^{-4}	16.5436	0.0827

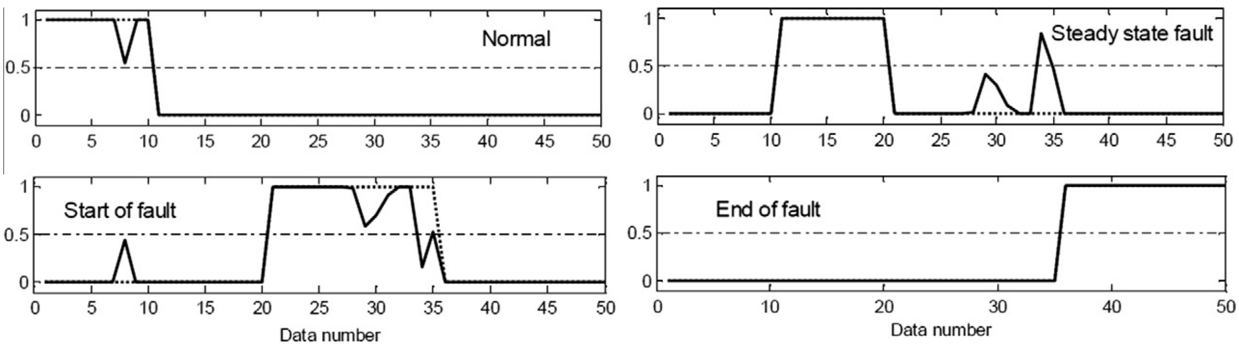

Fig. 15. Detection using feedforward neural network (dot line is a target, solid line is a detection).

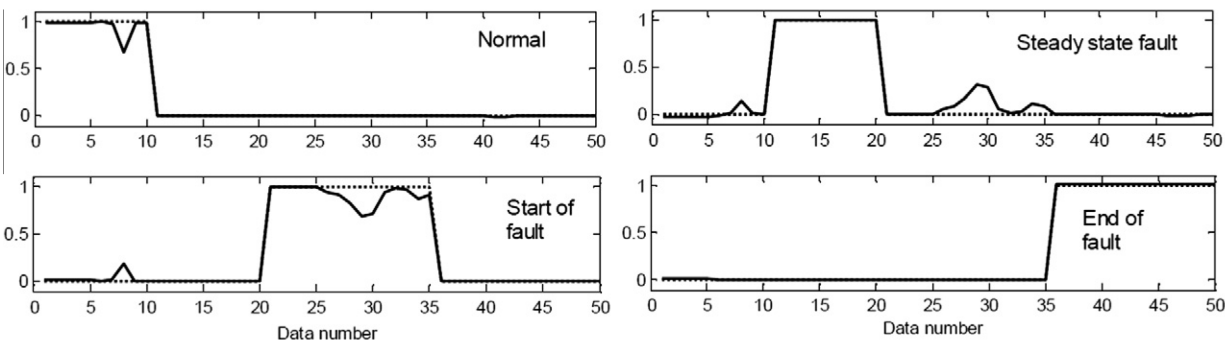

Fig. 16. Detection using Elman neural network (dot line is a target, solid line is a detection).

$$v_q(x) = \|x - C_q\| = \sqrt{\sum_{p=1}^{m} \left(x_p - c_{q,p}^2\right)}, \quad i = 1, 2, .., m \tag{26}$$

where $x = [x_1, x_2, \ldots, x_m]^T$, C_q is the center of the qth RBF unit, which is a vector whose dimension is equal to the number of inputs to the neuron q. The network architecture is shown in Fig. 5. The network output is formed by a linearly weighted sum of the number of basis functions in the hidden layer and can be calculated as follows.

$$y_r = \sum_{q=1}^{n} w_{qr} h_q \tag{27}$$

where y_r is the output of the rth node in the output layer, w_{qr} is the weight from the qth hidden layer neuron to the rth output layer

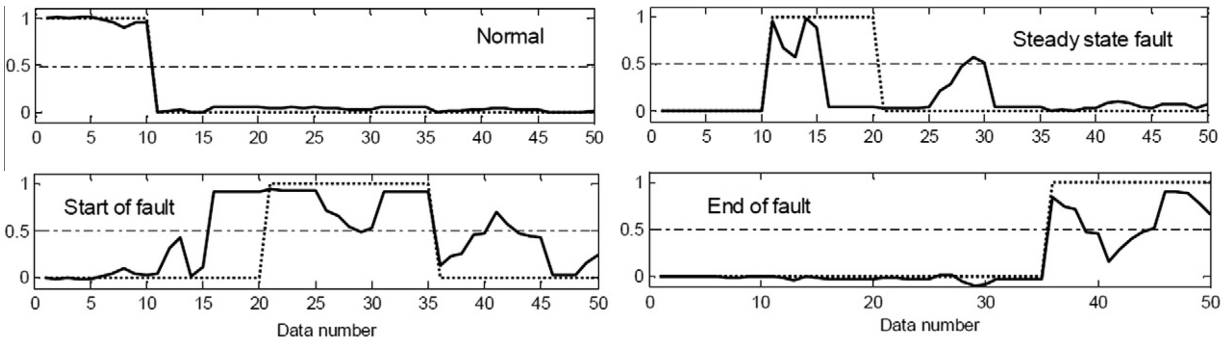

Fig. 17. Detection using RBF neural network (dot line is a target, solid line is a detection).

neuron, and h_q is the output of the qth node in the hidden layer (Zhang & Zhang, 2004).

3. Experimental set up and data generation

In this paper, laboratory scale experimental set up is performed consist of single phase induction motor 1/4 HP 1400 RPM, 50 Hz 110/220 V 4,8/2.4 A. Motor current is measured by Analog to Digital converter and storage oscilloscope with 1 kHz sampling frequency. Variable resistance is inserted in this scheme for varying the short circuit case with different fault current. Experimental scheme and setup are shown in Figs. 6 and 7 respectively. By using this set up, temporary short circuit is conducted and specified as short duration, less than 0.1 s and high impedance short circuit that produce low current short circuit, less than 300% power rating.

Transient period during short circuit starting and ending occur are recorded. This transient period is used to detect the short circuit occurrences in the proposed method. Fig. 8 shows the current signal spectrum during temporary short circuit. The short circuit starts at 103 ms and disappears at 175 ms, which means the duration of short circuit is 72 ms. In this cases short circuit current has low current level which has peak value of 4 A.

Figs. 9 and 10 show high frequency of faulty signal using first and second level wavelet respectively. As shown in those figures, the second level wavelet transform is more clearly able to distinguish the starting and ending points of fault. Fig. 11 shows the high frequency signal square of second level wavelet transform. The significant difference of magnitude value for normal and faulty cases is provided in this figure. Moreover, the square value is then used to energy level calculation in the next step. Fig. 12 shows the energy level graph in whole of signal in Fig. 8. Energy level is obtained using (18) which has period sampling is 10 ms or half cycle current waveform. As shown in this figure, the energy level during normal operation is mostly less than 0.1, but during fault period mostly more than 0.1. In addition, when the short circuit starting occurs, the energy level increases gradually from normal into fault and the opposite when the short circuit disappears, the energy level is decreased from fault to the normal. Fig. 13 shows the input variable $x1$, $x2$ and $x3$. Actually, these variables come from the same signal $x3$ but delayed by 20 ms and 10 ms for $x1$ and $x2$, respectively. When we concern to all of these three variables in the similar time, we can see that the normal condition is indicated by almost same low level of energy and fault condition is indicated by same high level energy. Moreover, transient starting short circuit is indicated by low, medium and high level energy for $x1$, $x2$ and $x3$, respectively. Conversely, the ending of short circuit has trends of high, medium and low level for $x1$, $x2$ and $x3$. By using this common trending approach, the neural network inputs are decided to be $x1$, $x2$ and $x3$.

In order to construct neural network detection system, 730 operating condition are recorded varied by short circuit current level. Data is divided into three following parts; training data, validation data and testing data. Training and validation data have similar short circuit level but they are different for testing data. The detail information about the data is shown in Table 1.

4. Neural network design

Feed forward, Elman and radial basis function neural networks are evaluated to achieve the best performance detection. Each type of neural network is designed as three layer networks consist of input layer, single hidden layer and output layer. Input layer and output layer consist of three and four nodes, respectively. In order to obtain most appropriate number of hidden node, various numbers of hidden nodes were tested. Fig. 14 shows the performance of the network as a function of number of hidden node and spread. The best performance of FFNN is achieved when number of hidden nodes is 7 and gives 0.0139 mean square error (MSE) of data test. On the other hand, ELMNN achieves the minimum MSE of 0.0034 with 5 hidden nodes and RBFNN optimum design is achieved with 0.022 and 00827 for spread and MSE, respectively.

Table 2 shows more detailed performance of best of design network each types. All of the investigated networks result in acceptable MSE value of data training. Better value of performance for data training is given by FFNN and RBF but for data test ELMNN gives the best result. This result concludes that ELMNN is more simply and accurately than other typical artificial neural networks for detection system of temporary short circuit fault. In other results, the RBFNN may produce the best MSE training process but not for data testing. It is due to the instability network during the validation process and also the overfitting condition of the network.

Table 3
Detection efficiency.

Network type	Normal		Steady state fault		Starting fault		Ending fault		Efficiency (%)
	TD	FD	TD	FD	TD	FD	TD	FD	
FFNN	49/50	1/50	48/50	2/50	48/50	2/50	50/50	0/50	97.5
ELMNN	50/50	0/50	50/50	0/50	50/50	0/50	50/50	0/50	100
RBFNN	50/50	0/50	47/50	3/50	35/50	15/50	43/50	7/50	87.5

5. Detection system analysis

Detection results of the selected neural network are presented in Figs. 15–17. Designed neural network has four outputs that presented four operating condition, normal, steady state fault, start of fault and end of fault. If motor running under normal operation, the value of first output is one and others output are zero. While steady state short circuit exists in motor winding, the second output value will be one and other outputs are zero. Furthermore, the outputs are (0 0 1 0) and (0 0 0 1) for starting and ending of fault, respectively.

Implementation the FFNN to 50 cases data test is shown in Fig. 15. The first output is the detected normal condition which should be resulted one for data number 1 until 15 and zero for data number 16–50. But as shown in Fig. 15, one case is false detection, case number 8 which resulted 0.5. Using threshold 0.5 to distinguish false and true detection, it can be summarized that one of 50 testing cases is false detection (FD) and 49 of 50 cases is true detection (TD). The summarized over all cases and network is presented in Table 3. Network efficiency is calculated as mean of TD. The best efficiency is given by ELMNN with almost 100% TD, while 97.5% and 87.5% for FFNN and RBFNN, respectively.

6. Conclusion

This paper describes the potential to combine the artificial neural network methods with wavelet transform approach to detect temporary short circuit in induction motor winding more accurately. Temporary short circuit is defined as short time occurrences and low current level short circuit. In this proposed method, detection based on transient starting and ending short circuit using energy level is presented. Energy level is obtained from high frequency signal of second level Haar wavelet transform. Experimental setup is performed to obtain 730 data set varied by short circuit level. These high energy levels are used as the input signals for developed and investigated artificial neural network. Three types of neural network, such as feed forward, Elman and radial basis function neural networks have been evaluated for fault detection system. Each network is designed using 3 input nodes, 4 output nodes and different optimal hidden layers. In order to obtain the best design of network, the number of hidden nodes and spread are tested and evaluated using Mean Square Error (MSE) value of unseen testing data. The result showed that Elman neural network with 5 hidden layers gives almost 100% accuracy of detection.

References

Acosta, G. G., Verucchi, C. J., & Gelso, E. R. (2006). A current monitoring system for diagnosing electrical failures in induction motors. *Mechanical Systems and Signal Processing, 20*, 953–965.

Burrus, C. S., Gophinath, R., & Guo, H. (1998). *Introduction to wavelet and wavelet transforms*. New Jersey: Prentice Hall.

Cusido, J., Rosero, J. A., Ortiga, J. A., Garcia, A., & Romeral, L. (2006). Induction motor fault detection by using wavelet decomposition on dq0 components. In *IEEE ISIE 2006, Montreal, Quebec, Canada* (pp. 2406–2411).

Cusido, J., Romeral, L., Ortega, J. A., Rosero, J. A., & Garcia Espinosa, A. (2008). Fault detection in induction machines using power spectral density in wavelet decomposition. *IEEE Transactions on Industrial Electronics, 55*(2), 633–643.

D'angelo, M. F. S. V., Palhares, R. M., Takahashi, R. H. C., Loschi, R. H., Baccarini, L. M. R., & Caminhas, W. M. (2011). Incipient fault detection in induction machine stator-winding using a fuzzy-Bayesian change point detection approach. *Applied Soft Computing, 11*(1), 179–192.

Kim, K., & Parlos, A. G. (2002). Model-based fault diagnosis of induction motors using nonstationary signal segmentation. *Mechanical System and Signal Processing, 16*, 223–253.

Kirmaci, V., Menlik, T., & Ozdemir, M. B. (2010). Determination of freeze-drying behaviors of apples by artificial neural network. *Expert Systems with Applications, 37*(12), 7669–7677.

Koker, R. (2006). Design and performance of an intelligent predictive controller for a six-degree-of-freedom robot using the Elman network. *Information Sciences, 176*(12), 1781–1799.

Niu, G., Widodo, A., Son, J. D., Yang, B. S., Hwang, D. H., & Kang, D. S. (2008). Decision-level fusion based on wavelet decomposition for induction motor fault diagnosis using transient current signal. *Expert Systems with Applications, 35*, 918–928.

Rodriguez, P. V. J., Negrea, M., & Arkkio, A. (2008). A simplified scheme for induction motor condition monitoring. *Mechanical Systems and Signal Processing, 22*(5), 1216–1236.

Sharif, S. S., & Taylor, J. H. (2000). Short-term load forecasting by feed-forward neural networks. In *Proceedings of the IEEE/ASME first international energy conference (IEC 2000), Al Ain, United Arab Emirates*. <http://www.ee.unb.ca/jtaylor/Publications/iec2000>.

Siddique, A., Yadava, G. S., & Singh, B. (2005). A review of stator fault monitoring techniques of induction motors. *IEEE Transactions on Energy Conversion, 20*(1), 106–114.

Tran, V. T., Yang, B. S., Oh, M. S., & Tan, A. (2009). Fault diagnosis of induction motor based on decision trees and adaptive neuro-fuzzy inference. *Expert Systems with Applications, 36*(2), 1840–1849.

Yang, B. S., Jeong, S. K., Oh, Y. M., & Tan, A. C. C. (2004). Case-based reasoning system with Petri nets for induction motor fault diagnosis. *Expert Systems with Applications, 27*(2), 301–311.

Zhang, A., & Zhang, L. (2004). RBF neural networks for the prediction of building interference effects. *Computers and Structures, 82*, 2333–2339.